



Long-Range Electron Tunneling

Jay R. Winkler* and Harry B. Gray*

Beckman Institute, California Institute of Technology, 1200 East California Boulevard, Pasadena, California 91125, United States

S Supporting Information

ABSTRACT: Electrons have so little mass that in less than a second they can tunnel through potential energy barriers that are several electron-volts high and several nanometers wide. Electron tunneling is a critical functional element in a broad spectrum of applications, ranging from semiconductor diodes to the photosynthetic and respiratory charge transport chains. Prior to the 1970s, chemists generally believed that reactants had to collide in order to effect a transformation. Experimental demonstrations that electrons can transfer between reactants separated by several nanometers led to a revision of the chemical reaction paradigm. Experimental investigations of electron exchange between redox partners separated by molecular bridges have elucidated many fundamental properties of these reactions, particularly the variation of rate constants with distance. Theoretical work has provided critical insights into the superexchange mechanism of electronic coupling between distant redox centers. Kinetics measurements have shown that electrons can tunnel about 2.5 nm through proteins on biologically relevant time scales. Longer-distance biological charge flow requires multiple electron tunneling steps through chains of redox cofactors. The range of phenomena that depends on long-range electron tunneling continues to expand, providing new challenges for both theory and experiment.

The propensity of light particles to tunnel through potential energy barriers was recognized early in the development of quantum mechanics. At first the phenomenon was exclusively the purview of physicists: in January 1928, Oppenheimer invoked electron tunneling (although not by name) through a potential barrier to explain electric-field-induced emission from atoms;¹ five months later, Fowler and Nordheim published their landmark work describing field-induced electron emission from cold metals;² in September 1928, Gurney and Condon rationalized α -particle decay in terms of tunneling;³ and two months later Gamow published a quantitative tunneling model that closely reproduced the empirical Geiger–Nuttall relationship between α -decay lifetime and particle energy.⁴

Solid-state physicists discovered the importance of tunneling in the middle of the 20th century. Many of the new devices developed by the rapidly expanding semiconductor electronics industry depended on electrons tunneling through potential energy barriers. In 1934, Clarence Zener formulated a theory of field-induced electron tunneling between energy bands in solid dielectrics.⁵ The semiconductor devices developed 15 years later at Bell laboratories appeared to exhibit this phenomenon,

leading William Shockley to name them Zener diodes.⁶ Later, Leo Esaki found that thin, heavily doped p – n junctions exhibited negative resistance in the low-voltage regime (tunnel diodes), a phenomenon readily explained by quantum mechanical tunneling of electrons through the junction.⁷ Today the physics of semiconductors is understood in great detail, owing to the vigorous interplay between theory and experiment that has occurred over many years. And, in recent years, the electronics industry has begun to move to the nanoscale to take advantage of groundbreaking work in conducting polymers,^{8–11} molecular wires,¹² and molecular electronic devices.^{13–16}

CHEMISTRY

In the final third of the 20th century, chemists began to explore the role of electron tunneling in reactions between molecular species. The semiclassical theory of electron-transfer (ET) (eq 1) reactions formulated by, *inter alia*, Marcus^{17,18} and Levich

$$k_{\text{ET}} = \sqrt{\frac{4\pi^3}{h^2 \lambda k_{\text{B}} T}} H_{\text{AB}}^2 \exp\left(-\frac{(\Delta G^\circ + \lambda)^2}{4\lambda k_{\text{B}} T}\right) \quad (1)$$

and Dogonadze¹⁹ provided a theoretical underpinning for countless experimental investigations. The theory expresses the specific rate of ET between two weakly interacting redox centers held at fixed distance and orientation in terms of the standard free-energy change for the reaction (ΔG°), a parameter describing the extent of nuclear reorientation and reorganization accompanying ET (λ), and the electronic coupling strength between reactants and products at the transition-state nuclear configuration (H_{AB}). The exponential factor reflects the probability of forming the activated complex for the reaction; H_{AB}^2 describes the probability of electron tunneling from donor to acceptor in the activated complex.

The Gaussian free-energy dependence of the specific rate is a unique feature of homogeneous ET reactions; in favorable cases, rates are observed to decrease as driving forces increase beyond λ (inverted effect, Figure 1). The fact that energy-saving charge-separation reactions in photosynthetic reaction centers are faster than energy-wasting recombination processes has been rationalized in terms of inverted effects.^{20,21} Often, however, inverted behavior is masked by the production of electronically excited products so that rates tend to plateau at high driving forces. Marcus recognized that chemiluminescent ET reactions are a manifestation of inverted driving-force effects.²² Rate-limiting diffusion of reactants in bimolecular ET

Received: January 8, 2014

Published: February 5, 2014



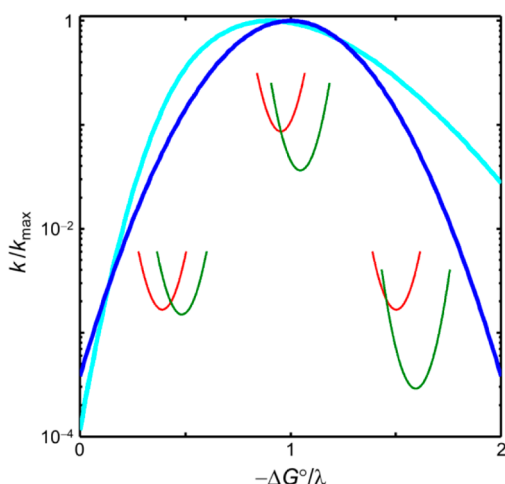


Figure 1. Theoretical driving-force dependence of electron-transfer reactions ($T = 295$ K). Classical treatment of nuclear rearrangements (blue) based on $\lambda = 0.8$ eV.¹⁸ The intersecting parabolas represent reactant (red) and product (green) potential energy surfaces along the reaction coordinate for normal (left), optimized (middle), and inverted (right) driving forces. A quantum mechanical treatment (cyan: one classical mode, $\lambda = 0.5$ eV; one quantum mode, $\lambda = 0.3$ eV; $\hbar\omega = 1500$ cm⁻¹) predicts damped inverted behavior.³²

reactions further frustrated the search for inverted behavior. The fluorescence quenching work of Rehm and Weller is likely the best known example of this phenomenon.²³ Because of these obstacles, some of the earliest observations of inverted driving-force effects were found in return ET reactions in photogenerated geminate radical pairs,²⁴ as well as in bimolecular return reactions.²⁵ Ultimately, molecules with electron donors and acceptors linked by covalent bonds were prepared, and ET kinetics measurements produced several unequivocal demonstrations of inverted behavior.^{26,27} The theory leading to eq 1 treats nuclear motions classically. Quantum mechanical refinements indicate that reorganization in high-frequency vibrational modes will substantially attenuate the magnitude of the inverted effect (Figure 1).^{28–32}

A common approach to overcome the diffusion problem involved immobilization of electron donors and acceptors in rigid solvents. Reactions were initiated pulse radiolytically³³ or photochemically,^{34–39} and kinetics were interpreted in terms of random distributions of redox partners.^{40–42} Two parameters were extracted from the data: a rate constant for ET at close

contact (k_{ET}^0); and an exponential distance decay constant β ($k_{\text{ET}} = k_{\text{ET}}^0 e^{-\beta(r-r_0)}$) that describes the efficiency of long-range coupling. In square-barrier tunneling models, β depends on the height of the barrier and the effective electron mass.⁴³ Although square-barrier tunneling models accurately predict the exponential distance dependence of long-range ET reactions, they provide no insight into how the properties of the bridging medium determine the coupling strength.

Superexchange tunneling models gained favor over geometric barrier models because they describe long-range couplings in terms of the electronic structure of the intervening medium. The theory of superexchange interactions, formulated first by Kramers⁴⁴ and later by Anderson,⁴⁵ rationalized interactions between magnetic centers separated by nonmagnetic ions. Halpern and Orgel generalized the superexchange theory to describe inner-sphere ET processes,⁴⁶ and McConnell used perturbation theory to elaborate the model for electron donor–acceptor molecules separated by an oligomeric bridge composed of j identical repeat units (Figure 2).⁴⁷ McConnell's familiar result (eq 2) describes H_{AB} in terms of the energy gap

$$H_{\text{AB}} = \frac{h_{\text{Db}}}{\Delta\epsilon} \left(\frac{h_{\text{bb}}}{\Delta\epsilon} \right)^{j-1} h_{\text{bA}} \quad (2)$$

between electron (or hole) states on the donor (or acceptor) and electron (or hole) states of the bridging medium ($\Delta\epsilon$) and the coupling strengths between the donor and the bridge hole or electron states (h_{Db}), the acceptor and the bridge states (h_{bA}), and adjacent bridge states (h_{bb}). The theory predicts that H_{AB} will be an exponential function of j and, hence, that rates will be exponential functions of donor–acceptor distance (r), in agreement with geometric barrier models. Taking the length of a bridge element as δ , the empirical distance decay constant can be defined in terms of superexchange parameters (eq 3).

$$\beta = -\frac{2}{\delta} \ln \left(\frac{h_{\text{bb}}}{\Delta\epsilon} \right) \quad (3)$$

Measurements of ET in rigid solvents are readily interpreted in terms of superexchange coupling models. Following work by Ponce,³⁸ Wenger found that β depended on the properties of the glass: 25% aqueous H₂SO₄, 16.0(5) nm⁻¹; 2-methyl-tetrahydrofuran (2-MTHF), 16.2(5) nm⁻¹; toluene, 12.3(5) nm⁻¹ (Figure 3).³⁹ The coupling efficiencies indicate that electron tunneling through 2.5 nm of toluene is several

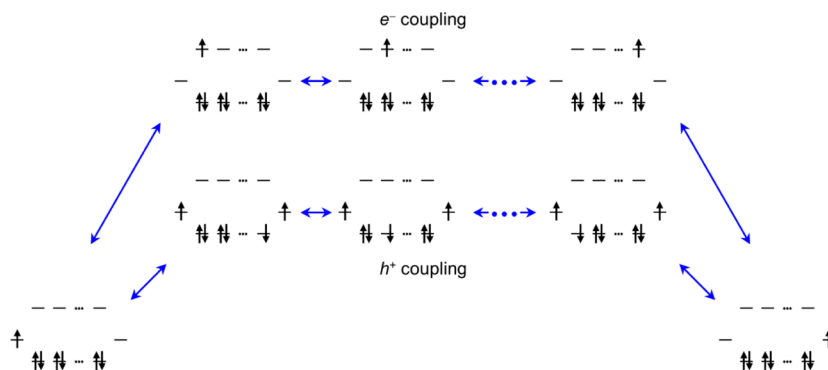


Figure 2. Orbital diagram representation of the states mediating electron-transfer superexchange coupling. The electron transfers from the orbital on the left to an equivalent one on the right. Electronic coupling can be mediated by excess electron (e^- coupling) or hole states (h^+ coupling) on the intervening bridge.

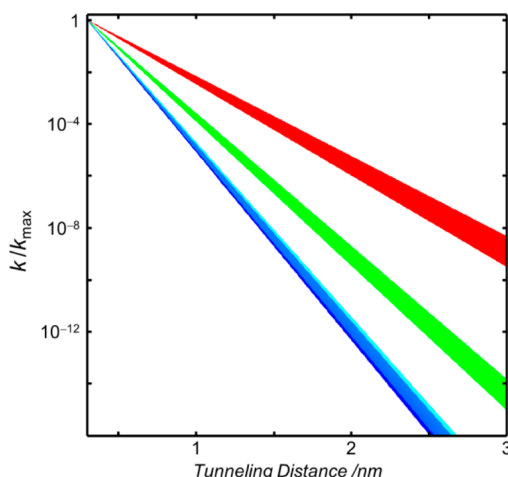


Figure 3. Distance dependence of rate constants for electron tunneling through solvent glasses (2-MTHF, blue; 25% aqueous H_2SO_4 , cyan; toluene, green) and across oligoxylene bridges (red).^{38,39}

thousand times faster than tunneling across the same distance in 2-MTHF or 25% aqueous H_2SO_4 . The smaller energy gaps ($\Delta\epsilon$) to electron or hole states of toluene, compared to the analogous gaps for 2-MTHF or 25% H_2SO_4 , likely account for the variation in β values. The decay constant for tunneling through an oligoxylene bridged donor–acceptor pair was found to be $7.6(5) \text{ nm}^{-1}$;³⁹ tunneling across 2.5 nm of this bridge would be over 10 000 times faster than tunneling through toluene. The likely explanation for this difference is that the coupling mediated by the C–C bond between xylene rings (h_{bb}) is substantially greater than that associated with van der Waals contacts between toluene molecules in the solvent glass.

The appealing simplicity of eqs 2 and 3 conceals some quantitative difficulties with the one-electron nearest-neighbor superexchange model. Several studies of ET across saturated alkane bridges,^{26,48–50} particularly in self-assembled monolayers (SAMs) of normal alkanes on gold electrodes, have produced β values of $\sim 10 \text{ nm}^{-1}$ (Figure 4).^{51–53} Taking $\delta = 0.154 \text{ nm}$ leads to the estimate $h_{\text{bb}}/\Delta\epsilon \approx 0.5$, a value that barely fulfills McConnell's perturbation theory requirements (i.e., $|h_{\text{bb}}/\Delta\epsilon| \ll 1$). Direct measurements of h_{bb} and $\Delta\epsilon$ are not feasible, but spectroscopic data can provide insights into their relative magnitudes. Estimates of energy gaps to hole states are relatively straightforward. The gas-phase ionization energies of saturated alkanes decrease as the number of carbon atoms increases: C_2H_6 , IE(adiabatic) = 11.52 eV; $\text{C}_{11}\text{H}_{24}$, 9.65 eV (Figure 5).^{54,55} This progression is consistent with modest delocalization of σ -bonding electrons as the carbon backbone lengthens. The ferricenium/ferrocene (Fc^+/Fc) redox couple was used in much of the alkane SAM work, and valence photoelectron spectra have been measured for this archetypal organometallic compound. The vertical ionization energy of Fc is 6.88 eV,⁵⁶ but this is not the quantity of interest. Since the electronic coupling matrix element in eq 1 corresponds to the transition-state nuclear configuration, the adiabatic ionization energy ($\sim 6.65 \text{ eV}$)⁵⁶ is more appropriate (Supporting Information). Consequently, the gas-phase energy gaps for Fc^+/Fc hole tunneling across alkane spacers ($n\text{-C}_j\text{H}_{2j+2}$, $j = 5\text{--}11$) range from 3.6 to 2.9 eV.

In condensed phases, the energy gaps are likely to shift somewhat, owing to polarization of the surrounding medium.

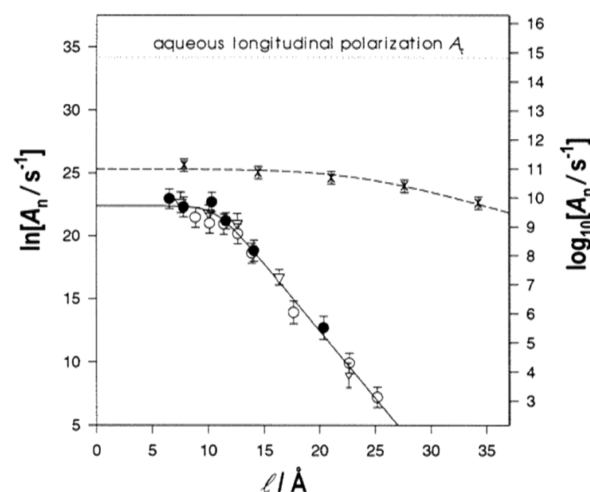


Figure 4. Distance dependence of Arrhenius prefactors for electron-transfer reactions between a Au electrode and redox couples attached to the termini of oligomethylene (directly linked Fc, ●; ester-linked Fc, ○; $\text{Ru}(\text{pyridine})(\text{NH}_3)_5^{2+}$, ▽) and oligovinylene (×) spacers. For distances $>12 \text{ Å}$ (1.2 nm), oligomethylene rates are described by an exponential distance decay of 10.6 nm^{-1} (solid line). The dotted line shows the prefactor expected for reactions limited by solvent dynamics. Reprinted with permission from ref 51. Copyright 2003 American Chemical Society.

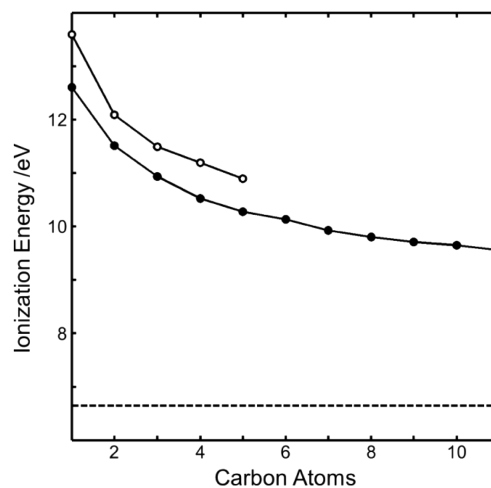


Figure 5. Gas-phase vertical (○) and adiabatic (●) ionization energies for normal saturated hydrocarbons.^{54,55} The dashed line corresponds to the adiabatic ionization energy of ferrocene.⁵⁶

Photoconductivity measurements indicate that ionization thresholds of saturated hydrocarbons decrease by about 1.5 eV upon moving from gas to liquid phases.⁵⁷ The binding energy of the tunneling electron for the ferricenium/ferrocene redox couple ($E^\circ = 0.4 \text{ V}$ vs NHE)⁵⁸ is near 4.9 eV, suggesting that $\Delta\epsilon$ is in the range of 3.9–3.1 eV for condensed-phase, normal alkane bridges.

Estimation of energy gaps for electron tunneling is more problematic. A naïve approach involves estimation of the LUMO energy of a molecular bridge on the basis of its absorption and ionization spectra. The onset of far-UV absorption in gaseous and liquid normal alkanes ($n\text{-C}_j\text{H}_{2j+2}$, $j = 5\text{--}14$) is near 8 eV.^{59–63} The maxima found in liquids between 8.45 and 8.18 eV, and the shoulders near 7.7 eV, have been assigned to electronic excitations of σ -bonding electrons into Rydberg-type orbitals (3p and 3s, respectively).⁶³ Taking

7.7 eV for the HOMO–LUMO energy gap, along with the gas-phase ionization energies of saturated alkanes, places LUMO energies 2.6–1.9 eV below the vacuum level.

The diabatic states that would mediate coupling for ET, however, do not correlate directly with those observed in valence-shell or Rydberg absorption spectra. The appropriate states for electron tunneling are anion states of the bridging molecule.⁶⁴ In an *m*-electron molecule, the electron promoted to the LUMO in a valence-shell excited state sees an effective potential produced by *m* – 1 electrons. The effective potential seen by the excess electron in an anion created from an *m*-electron parent, however, is produced by *m* electrons. The consequence is that the extra electrons in anions are very weakly bound, or not even bound at all. Indeed, negative electron affinities are extracted from resonances in electron transmission spectra (ETS) of many organic molecules.^{65,66} Only very broad (~4–5 eV) ETS resonances, indicative of extremely short-lived anion states, have been detected in the 7–9 eV range for saturated alkanes.⁶⁷ States so far above the vacuum level seem unlikely to assist long-range electronic coupling between donors and acceptors separated by alkane spacers.

Ab initio calculations of gas-phase electronic couplings across saturated alkane spacers provide interesting comparisons to the experimental quantities.^{68–70} In a Natural Bond Orbital (NBO) basis,^{71,72} intrabridge coupling elements (h_{bb}) between C–C σ -bonding orbitals in *trans*-*n*-alkane spacers are estimated to be ~2.7 eV.^{68,69} The energy gaps depend on the redox partner chosen for the calculations. For alkane-bridged methylene cation and anion radicals ($[\text{H}_2\text{C}-(\text{CH}_2)_j-\text{CH}_2]^\pm$), $\Delta\epsilon$ values of ~8 eV emerged from the calculations for both hole tunneling in the cations and electron tunneling in the anions.^{68,69} Experimental data suggest a somewhat smaller gap for hole tunneling: the vertical ionization energy of the ethyl radical ($\text{H}_3\text{C}-\text{CH}_2^\bullet$) is 8.1 eV; its electron affinity is –0.26 eV.^{73–75} Substituting the theoretical values in eq 3 would suggest $\beta \approx 14 \text{ nm}^{-1}$, but the full calculation gave $\beta \approx 5\text{--}7 \text{ nm}^{-1}$ for transfer in $[\text{H}_2\text{C}-(\text{CH}_2)_j-\text{CH}_2]^\pm$.⁶⁹ Clearly, the McConnell model does not capture all contributions to the coupling matrix element; a principal source of the discrepancy lies in the inclusion of only nearest-neighbor interactions. Ratner demonstrated that the McConnell model could be generalized to give H_{AB} as a sum of the contributions from all pathways.⁷⁶ Since the coupling is a signed quantity, this extended McConnell model admitted the possibility of constructive and destructive interference from competing coupling routes. *Ab initio* calculations of coupling along *trans*-*n*-alkane spacers revealed that non-nearest-neighbor coupling pathways make substantial constructive contributions to the total coupling between donors and acceptors.^{68–70} Moreover, pathways involving antibonding orbitals of the alkane contributed to the calculated couplings for the cations; H_{AB} was neither exclusively hole nor electron mediated. These studies indicated that although nearest-neighbor McConnell pathways did not lead to accurate estimates of long-range couplings, more coarsely grained effective pathways based on larger repeat units could be represented by a McConnell-type model.⁶⁹

The energy gaps to hole and electron states of saturated alkane bridges are extremely large for most conventional redox reagents. The same cannot be said for many unsaturated hydrocarbon bridges. Moreover, the decrease in energy gap with increasing bridge length complicates analyses of distance dependences. When the energy gaps become small, incoherent

hopping through real redox intermediates begins to compete with coherent single-step long-range tunneling.^{77–79} Wasielewski and co-workers demonstrated that ET across oligo-*p*-phenylenevinylene bridges ($\beta_{\text{obsd}} = 0.4 \text{ nm}^{-1}$) is a case in point.^{77,78} Analysis of the temperature dependences of these kinetics suggested that hopping is gated by torsional motions involving the donor and the bridge. A similarly shallow distance dependence ($\beta_{\text{obsd}} = 0.6 \text{ nm}^{-1}$) was reported for tunneling from a gold electrode to the Fc^+/Fc couple across SAMs composed of oligo-*p*-phenylenevinylene bridges. In this instance, estimated energy gaps (>1 eV) are larger than observed activation energies (~0.2 eV), and incoherent hopping was ruled out.⁵³ Instead, the weak distance dependence was attributed to dynamically limited, adiabatic ET. It is apparent that the empirical β values for ET across oligo-*p*-phenylenevinylene bridges in both the small and large energy gap regimes are too small to be consistent with superexchange-mediated tunneling. The surprising finding is that two different mechanisms appear to be responsible for virtually distance-independent transport across this bridge.

■ BIOLOGY

Understanding electron transfer in biological systems has challenged chemists for over half a century. Szent-Györgyi, in attempting to rationalize electron transport in respiratory chains, suggested that electrons move among enzymes in energy bands, analogous to transport in semiconductors.⁸⁰ This proposal met considerable opposition,^{81–83} although no suitable alternative appeared for more than 25 years. In 1966, DeVault and Chance reported that rates of cytochrome oxidation in flash-irradiated suspensions of photosynthetic bacteria reached a limiting value ($\tau \approx 2 \text{ ms}$) as the temperature decreased below 100 K; they suggested that quantum mechanical tunneling was the explanation.⁸⁴ Without structural information and a precise understanding of the ET reaction, little more could be concluded. Eight years later, Hopfield developed a thermally activated tunneling model to describe the DeVault and Chance data.⁸⁵ He postulated a 2 eV barrier height, leading to a 14.4 nm^{-1} distance decay constant and a predicted 0.8 nm tunneling distance.

Definitive evidence for long-range electron tunneling through proteins emerged in 1982 from our work on cytochrome *c* modified with a $\text{Ru}^{\text{III}}(\text{NH}_3)_5$ moiety coordinated to His33 on the protein surface ($\text{Ru}(\text{His33})\text{-Fe-cyt } c$).⁸⁶ In a kinetics study, flash photochemical electron injection generated transient $\text{Ru}^{\text{II}}(\text{His33})\text{-Fe}^{\text{III}}\text{-cyt } c$ that relaxed to the $\text{Ru}^{\text{III}}\text{-Fe}^{\text{II}}$ thermodynamic product with a time constant of 30 ms ($-\Delta G^\circ = 0.2 \text{ eV}$). Structural models placed the ET distance at 1.8 nm; tunneling was the only plausible explanation. Irrefutable evidence of long-range tunneling was provided by measurements of intramolecular ET reactions in protein crystals.^{87–89} The advent of site-directed mutagenesis and several experimental refinements developed over the ensuing years ultimately produced an experimentally validated timetable for long-range electron tunneling through proteins (Figure 6).^{90–92} We have measured the kinetics of high-driving-force ET in more than 30 Ru-labeled proteins: donor–acceptor distances vary from 1.2 to 2.6 nm, and specific rates span 7 orders of magnitude (10^9 to 10^2 s^{-1}). Driving-force-optimized rate constants are dispersed around an exponential distance decay of 11 nm^{-1} , but the substantial scatter reflects important features of the protein medium.^{90–94}

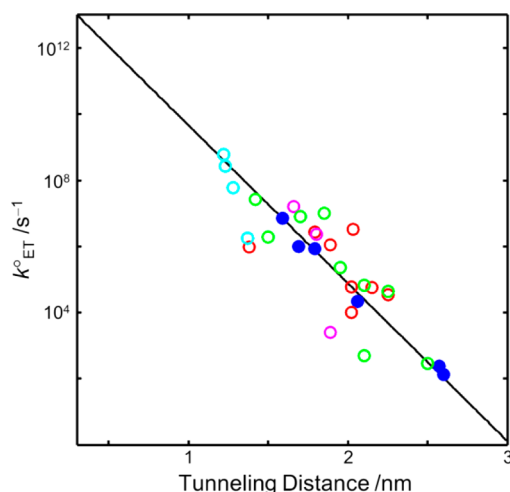


Figure 6. Distance dependence of driving-force-optimized ET rate constants for Ru-modified proteins: azurin (blue), cytochrome *c* (red), myoglobin (magenta), cytochrome *b*₅₆₂ (green), and high-potential iron protein (cyan).⁹⁰

A comparison between the distance dependence of ET through *n*-alkane spacers embedded in SAMs and that of Ru-proteins is illuminating. Arrhenius prefactors (roughly equivalent to driving-force-optimized homogeneous rate constants) for 10 ET rate measurements across *n*-alkanes in SAMs vary over 6 orders of magnitude (10^9 to 10^3 s⁻¹) in the 1.2–2.5 nm distance range, with a nearly perfect exponential distance dependence ($\beta = 10.6$ nm⁻¹).⁵³ The standard deviation for SAM data is less than a factor of 2 (1.8), whereas that for the Ru-protein data is a factor of 8. Clearly, the *n*-alkane spacers embedded in SAMs are extremely well-ordered structures that create a uniform barrier to long-range tunneling. Within the Ru-protein data set are examples where rate constants differ by a factor of 10^3 at the same donor–acceptor distance, and virtually identical rates are found for distances differing by 0.5 nm.^{90–92} The inescapable conclusion to be drawn from the protein data is that folded polypeptide matrices do not create a uniform barrier to electron tunneling. This conclusion is entirely consistent with investigations of electron tunneling through solvent glasses. Long-range coupling efficiencies are sensitive functions of the chemical composition of the glass ($\beta_{\text{toluene}} < \beta_{\text{H}_2\text{SO}_4} \approx \beta_{\text{2-MTHF}}$), and covalent linkages are superior to van der Waals contacts ($\beta_{\text{oligoxylylene}} < \beta_{\text{toluene}}$).³⁹

The side chains of the 20 amino acids have widely varying molecular and electronic structures, and polypeptide folds create a heterogeneous array of bonded and nonbonded contacts between electron donors and acceptors. When redox partners are oriented along an extended polypeptide, as they are in a β -sheet protein, Ru-azurin, ET rates exhibit a simple exponential distance dependence.^{90–92} However, donor–acceptor couplings mediated by side-chain atoms, hydrogen bonds, and van der Waals contacts will not depend solely on the separation distance; the structure and composition of the intervening medium will play a defining role. Understanding the long-range coupling in a protein, then, is a challenging quantum chemical problem involving a very small energy splitting between reactant and product states ($H_{\text{AB}} < 10$ cm⁻¹) composed of hundreds or thousands of atoms, with multiple coupling modes, interferences, conformational dynamics, and potential breakdown of the Born–Oppenheimer and Condon approximations.^{95–105} Nevertheless, *ab initio* electronic struc-

ture methods combined with molecular dynamics simulations have produced impressive strides in calculations of absolute ET rates in Ru-modified azurins.^{99,106} A great deal of fundamental information is subsumed in the calculation of protein ET rates. A decomposition of the calculated rates into contributions from electron and hole tunneling, and identification of the pathways contributing to the overall coupling, would be especially illuminating.^{13,107}

Two general principles that emerge from studies of ET in glasses can provide insights into the factors that control long-range biological ET reactions: aromatics are better than alkanes, and covalent bonds are superior to van der Waals contacts. As efficient long-range ET in DNA ($\beta < 10$ nm⁻¹) is facilitated by the high concentration of aromatic bases stacked in the double helix,^{108–110} we anticipate that aromatic amino acids will provide smaller tunneling energy gaps than aliphatic residues in proteins. In support of this view, the ionization energies of aliphatic amino acids (~ 9.6 eV) are greater than those of aromatic amino acids (Phe, 9.4(1) eV; Tyr, 8.5(1); Trp, 7.8(1)).^{111–113} Vertical electron attachment energies of Phe (0.87 eV) and Trp (0.68 eV) are about 1 eV less than those of Ala and Gly (1.80 and 1.93 eV, respectively).¹¹⁴ Assessing the biological implications of the second principle is a difficult prospect, because it requires knowledge of individual protein structures and, in the case of interprotein ET, encounter-complex structures.

With the ready accessibility of protein-sequence databases, it is possible to investigate whether biological ET reactions exploit the presumed greater coupling efficiency of aromatic amino acids. The four aromatic amino acids are among the least frequently occurring residues in the UniProtKB/Swiss-Prot protein sequence database¹¹⁵ (Phe, 3.90% of all residues, rank = 14; Tyr, 3.00%, 16; His, 2.36%, 18; Trp, 1.13%, 20) and have long been believed to stabilize folded structures, with additional roles in protein–protein recognition and ligand binding.^{116–119} Histidine has additional functional importance, owing to its basicity and preference for metal binding and, for the purposes of the subsequent discussion, is not included in the aromatic class. The average amino-acid frequencies of occurrence in proteins from the six enzyme classes (oxidoreductases, 37,408 sequences; transferases, 89,489; hydrolases, 61,743; lyases, 23,052; isomerases, 14,067; ligases, 30,513) defined by the Enzyme Data Bank of the Swiss Institute of Bioinformatics are illustrated in Figure 7. The striking feature in this comparison is that only among the oxidoreductases do aromatic residues appear more frequently than the database average. With the exception of Tyr in the ligases, aromatic amino acids occur substantially less frequently than database averages in the other five enzyme classes. Analyses of transmembrane protein structures reveal that aromatic amino acids are found preferentially in membrane interface regions; this trend is believed to enhance stability.^{120–122} Separate comparisons of amino acid frequencies in transmembrane and soluble proteins still exhibit higher frequencies of aromatics among the oxidoreductases, although the remaining five enzyme classes show some interesting variations (see Supporting Information). An obvious explanation for the higher frequencies of aromatic amino acids in oxidoreductases is their superior capability to mediate long-range ET. Testing this hypothesis is a challenging prospect—folded polypeptide structures will not tolerate wholesale exchange of aromatic and aliphatic residues. Analyses of the structures and ET properties of proteins with particularly high and low aromatic frequencies might provide some insight

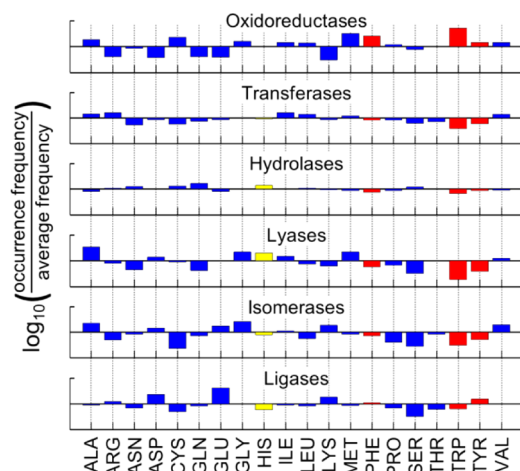


Figure 7. Amino acid occurrence frequencies in the primary sequences of six enzyme classes (oxidoreductases, 37,408 sequences; transferases, 89,489; hydrolases, 61,743; lyases, 23,052; isomerases, 14,067; ligases, 30,513) relative to the average frequencies in the Enzyme Data Bank of the Swiss Institute of Bioinformatics.¹¹⁵ All bar graphs have identical vertical axis limits (± 0.1).

into this question. The cytochromes P450 are a case in point (Figure 8): the average Phe occurrence frequency in the P450

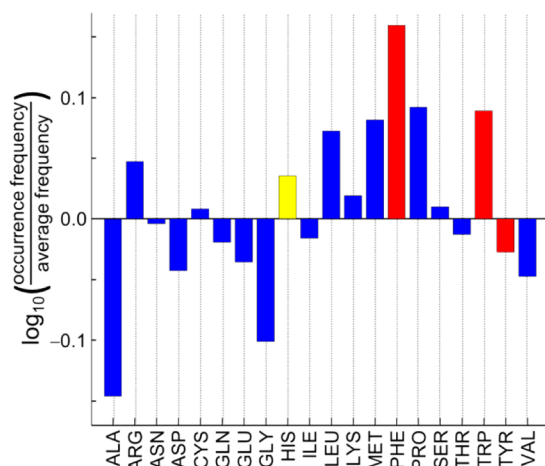


Figure 8. Amino acid occurrence frequencies in the primary sequences of the cytochrome P450 family of enzymes (975 sequences) relative to the average frequencies in the Enzyme Data Bank of the Swiss Institute of Bioinformatics.¹¹⁵

family is 45% greater than in the database as a whole; Trp frequencies are higher by 22%. Enhanced superexchange coupling between redox partners and the heme is one rationale for the prevalence of aromatics in this enzyme family.

The exigencies of biological function typically require that electrons be transferred in milliseconds over distances of 5 nm or more, yet it is clear from Figure 6 that single-step ET reactions across more than 2.5 nm cannot keep up with this pace. The solution to the problem is multistep tunneling (hopping): redox centers spaced at ~ 1.5 nm intervals with formal potentials near those of the terminal donors and acceptors.^{94,123,124} Indeed, it is likely that the 2 μ s cytochrome oxidation in *Chromatium vinosum* studied by DeVault and Chance in 1966, and analyzed theoretically by Hopfield in 1974, was a two-step tunneling reaction.¹²⁵ The structure of the

photosynthetic reaction center in *Chromatium* has not been determined, but the *Blastochloris viridis* (formerly *Rhodospirillum rubrum*) enzyme has an analogous string of four cytochromes^{126,127} [c_{554} , $E^\circ(\text{Fe}^{\text{III/II}}) = -0.07$ V vs NHE; c_{556} , $E^\circ = 0.32(1)$ V; c_{552} , $E^\circ = 0.02(1)$ V; c_{559} , $E^\circ = 0.38(1)$ V] that deliver electrons to the oxidized bacteriochlorophyll special pair [P^+ , $E^\circ(\text{P}^{+/0}) = 0.5$ V].^{125,128,129} The kinetics of P^+ reduction in two-electron-reduced ($\text{Fe}^{\text{II}}\text{-}c_{556}$, $\text{Fe}^{\text{II}}\text{-}c_{559}$) *B. viridis* reaction centers are biphasic: a 200 ns phase has been assigned to $\text{Fe}^{\text{II}}\text{-}c_{559} \rightarrow \text{P}^+$ ET, and a 2 μ s process is attributed to $\text{Fe}^{\text{II}}\text{-}c_{556} \rightarrow \text{Fe}^{\text{III}}\text{-}c_{559}$ ET.^{125,130} The Fe–Fe distance between c_{556} and c_{559} is 2.78 nm (PDB 2ISN),¹³¹ too far for a 2- μ s single-step ET reaction. Cytochrome c_{552} lies between c_{556} and c_{559} , with Fe–Fe distances of 1.65 ($c_{556}\text{--}c_{552}$) and 1.39 nm ($c_{552}\text{--}c_{559}$). EPR measurements indicate that the Fe^{III} hemes in c_{554} , c_{556} , and c_{552} are strongly coupled. Owing to electrostatic interactions among the cytochromes, it is difficult to determine precisely the driving forces for $\text{Fe}^{\text{II}}\text{-}c_{556} \rightarrow \text{Fe}^{\text{III}}\text{-}c_{552}$ and $\text{Fe}^{\text{II}}\text{-}c_{552} \rightarrow \text{Fe}^{\text{III}}\text{-}c_{559}$ ET reactions, but, on the basis of formal potentials extracted from redox titrations, it is likely that the two-step transfer from $\text{Fe}^{\text{II}}\text{-}c_{556}$ to $\text{Fe}^{\text{III}}\text{-}c_{559}$ involves an endergonic first step and a spontaneous second step.^{128,129} Redox chains that facilitate charge separation across biological membranes have been identified in several components of the photosynthetic and respiratory machinery.^{94,128,132}

Multistep biological electron tunneling need not always depend on redox-active metallo-cofactors. Perhaps the best-known example is the Class I ribonucleotide reductase in which a hole resides on a stable Tyr122 radical in the resting state of the *Escherichia coli* enzyme.^{133–142} A chain of Tyr and Trp residues is believed to mediate ET from an active-site Cys439 residue to Tyr122 \cdot over a distance of more than 3.5 nm. Multistep ET reactions via Trp and Tyr have been identified in several other natural systems: photosystem II,^{143–146} DNA photolyase,^{147–155} MauG,^{156–159} and the cytochrome *c*/cytochrome *c* peroxidase pair.^{160,161}

The natural hopping systems are not as amenable to systematic variations as are sensitizer-modified proteins. We examined the fundamental principles of multistep tunneling in a Re-modified azurin mutant engineered to have a Trp directly between Re and Cu centers separated by 1.9 nm. Cu^{I} oxidation by electronically excited Re^{I} was accelerated by a factor of more than 100 in this mutant; replacement of Trp by Tyr or Phe inhibited Cu^{I} oxidation.¹⁶² Hopping maps based on semiclassical ET theory have been used to identify potential locations for redox intermediates (Int) in Ru-modified azurins.¹⁶³ The greatest hopping advantage is predicted for azurins in which the Int– Ru^{III} distance is up to 0.5 nm shorter than that for Int– Cu^{I} . The hopping advantage increases as systems orient nearer a “straight line” between the donor and acceptor, a consequence of minimizing intermediate tunneling distances. The smallest predicted hopping advantage occurs when the Ru–Cu distance is less than 2 nm. Analyses of ET kinetics measurements in three Cu^{I} –Int– Ru^{III} azurins (Int = nitrotyrosinate) revealed that hopping via $\text{NO}_2\text{-TyrO}^\bullet$ accelerates Cu^{I} oxidation by factors of $\sim 10\text{--}50$, results that are fully consistent with the predictions of semiclassical theory.¹⁶³

Generation of oxidized Trp and Tyr radicals requires high-potential oxidants ($E^\circ > 1$ V vs NHE), so that they are likely to participate only in a relatively small subset of enzymatic transformations. The enzymatic reactions in which oxygen serves as an electron acceptor typically involve high-potential

intermediates. Examination of the amino-acid occurrence frequencies in O_2 - and H_2O_2 -reactive oxidoreductases (7149 sequences) reveals that Trp and Tyr are found much more often than the database average (Figure 9; see Supporting

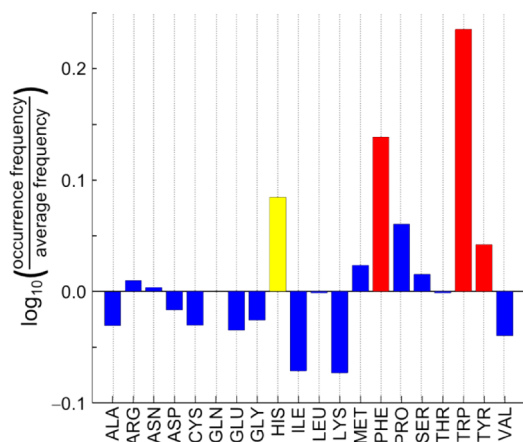


Figure 9. Amino acid occurrence frequencies in the primary sequences of O_2 - and H_2O_2 -reactive oxidoreductases (7149 sequences) relative to the average frequencies in the Enzyme Data Bank of the Swiss Institute of Bioinformatics.¹¹⁵

Information for additional comparisons). The involvement of Trp and Tyr radicals in ET reactions is one explanation for the prevalence of these residues in this class of enzymes. We speculate that, in addition to participation in on-pathway ET chains, Trp and Tyr radicals also might play protective roles in O_2 -reactive oxidoreductases. If these enzymes do not operate with high fidelity or if xenobiotics inhibit natural function, the high-potential intermediates generated during turnover can produce reactive species that damage and inactivate enzymes.^{164–166} Appropriately placed Tyr and/or Trp residues could prevent this damage by reducing the intermediates and directing the oxidizing hole to less harmful sites or out of the protein altogether. Devising methods to identify and detect protective biochemical mechanisms of this sort is an ongoing research challenge in biological ET.¹⁶⁷

■ HOW FAR CAN THEY GO?

Tremendous advances in theory and experiment during the past half-century have produced a rigorous foundation for understanding long-range electron transfers in chemistry and biology. Yet, many fundamental problems remain to be solved. Superexchange is generally agreed to be the dominant, but not exclusive, coupling mechanism for long-range ET, although the mediating states and energy gaps are rarely identified,^{13,107,168} nor are they correlated with the spectroscopic and thermodynamic properties of the bridging medium. Indeed, the uncertainty about energy gaps often leads to confusion about competition between coherent tunneling and incoherent hopping.

Empirical studies of long-range electron transport continue to challenge the current paradigm. A particularly interesting example is provided by bacterial nanowires. Groups of microbes are known that transfer electrons to extracellular Fe^{III} oxides.¹⁶⁹ Many of these bacteria contact the oxides via micrometer-long hairlike appendages known as pili. Some pili are coated with multiheme c -type cytochromes that have been suggested to serve as hopping intermediates in micrometer-distance

electron-transport processes.¹⁷⁰ Alternative interpretations, however, suggest that the pilus itself has metal-like conductive properties in the absence of the cytochromes.¹⁷¹ Beratan and co-workers have pointed out that superexchange tunneling theories impose severe constraints on these hyper-long-range ET processes.¹⁷² New insights into the ET properties of pili continue to emerge, but it remains to be clearly determined how this remarkable transport of electrons is accomplished.

■ ASSOCIATED CONTENT

Supporting Information

Estimation of the gas-phase Fc^+/Fc electron exchange tunneling energy and additional comparisons of amino acid occurrence frequencies. This material is available free of charge via the Internet at <http://pubs.acs.org>.

■ AUTHOR INFORMATION

Corresponding Authors

winklerj@caltech.edu

hbgray@caltech.edu

Notes

The authors declare no competing financial interest.

■ ACKNOWLEDGMENTS

Our electron transfer research is supported by the National Institutes of Health (DK-019038), the National Science Foundation (CHE-1305124), the Gordon and Betty Moore Foundation, and the Arnold and Mabel Beckman Foundation.

■ REFERENCES

- (1) Oppenheimer, J. R. *Phys. Rev.* **1928**, *31*, 66–81.
- (2) Fowler, R. H.; Nordheim, L. *Proc. R. Soc. London A* **1928**, *119*, 173–181.
- (3) Gurney, R. W.; Condon, E. U. *Nature* **1928**, *122*, 439.
- (4) Gamow, G. *Nature* **1928**, *122*, 805–806.
- (5) Zener, C. *Proc. R. Soc. London A* **1934**, *145*, 523–529.
- (6) It was later discovered that the breakdown properties of these devices arose not from field-induced tunneling but from avalanche breakdown. Diodes operating according to Zener's model were developed later: Morton, D. L.; Gabriel, J. *Electronics: The Life Story of a Technology*; Johns Hopkins University Press: Baltimore, 2007.
- (7) Esaki, L. *Phys. Rev.* **1958**, *109*, 603–604.
- (8) Shirakawa, H. *Angew. Chem., Int. Ed.* **2001**, *40*, 2575–2580.
- (9) MacDiarmid, A. G. *Angew. Chem., Int. Ed.* **2001**, *40*, 2581–2590.
- (10) Heeger, A. J. *Angew. Chem., Int. Ed.* **2001**, *40*, 2591–2611.
- (11) Hutchison, G. R.; Ratner, M. A.; Marks, T. J. *J. Phys. Chem. B* **2005**, *109*, 3126–3138.
- (12) Weiss, E. A.; Wasielewski, M. R.; Ratner, M. A. In *Molecular Wires: From Design to Properties*; DeCola, L., Ed.; Topics in Current Chemistry **257**; Springer: Berlin, 2005; pp 103–133.
- (13) Solomon, G. C.; Bergfield, J. P.; Stafford, C. A.; Ratner, M. A. *Beilstein J. Nanotechnol.* **2011**, *2*, 862–871.
- (14) Ratner, M. *Nat. Nanotechnol.* **2013**, *8*, 378–381.
- (15) Renaud, N.; Hliwa, M.; Joachim, C. In *Unimolecular and Supramolecular Electronics II: Chemistry and Physics Meet at Metal–Molecule Interfaces*; Mezger, R. M., Ed.; Topics in Current Chemistry **313**; Springer: Berlin, 2012; pp 217–268.
- (16) Li, C.; Mishchenko, A.; Wandlowski, T. *Unimolecular and Supramolecular Electronics II: Chemistry and Physics Meet at Metal–Molecule Interfaces*; Mezger, R. M., Ed.; Topics in Current Chemistry **313**; Springer: Berlin, 2012; pp 121–188.
- (17) Marcus, R. A. *J. Chem. Phys.* **1956**, *24*, 966–978.
- (18) Marcus, R. A.; Sutin, N. *Biochim. Biophys. Acta* **1985**, *811*, 265–322.

- (19) Levich, V. G.; Dogonadze, R. R. *Dokl. Akad. Nauk SSSR* **1959**, 124, 123–126.
- (20) Volk, M.; Aumeier, G.; Langenbacher, T.; Feick, R.; Ogrodnik, A.; Michel-Beyerle, M.-E. *J. Phys. Chem. B* **1998**, 102, 735–751.
- (21) Bixon, M.; Jortner, J. *J. Phys. Chem.* **1991**, 95, 1941–1944.
- (22) Marcus, R. A. *J. Chem. Phys.* **1965**, 43, 2654–2657.
- (23) Rehm, D.; Weller, A. *Isr. J. Chem.* **1970**, 8, 259–271.
- (24) Gould, I. R.; Ege, D.; Mattes, S. L.; Farid, S. *J. Am. Chem. Soc.* **1987**, 109, 3794–3796.
- (25) McCleskey, T. M.; Winkler, J. R.; Gray, H. B. *J. Am. Chem. Soc.* **1992**, 114, 6935–6937.
- (26) Closs, G. L.; Calcaterra, L. T.; Green, N. J.; Penfield, K. W.; Miller, J. R. *J. Phys. Chem.* **1986**, 90, 3673–3683.
- (27) Fox, L. S.; Kozik, M.; Winkler, J. R.; Gray, H. B. *Science* **1990**, 247, 1069–1071.
- (28) Jortner, J. *J. Chem. Phys.* **1976**, 64, 4860–4867.
- (29) Dogonadze, R. R.; Kuznetsov, A. M.; Vorotyntsev, M. A. *Phys. Status Solidi B* **1972**, 54, 125–134.
- (30) Dogonadze, R. R.; Kuznetsov, A. M.; Vorotyntsev, M. A. *Phys. Status Solidi B* **1972**, 54, 425–433.
- (31) Ulstrup, J.; Jortner, J. *J. Chem. Phys.* **1975**, 63, 4358–4368.
- (32) Brunschwig, B. S.; Sutin, N. *Comments Inorg. Chem.* **1987**, 6, 209–235.
- (33) Miller, J. R. *Science* **1975**, 189, 221–222.
- (34) Miller, J. R.; Hartman, K. W.; Abrash, S. *J. Am. Chem. Soc.* **1982**, 104, 4296–4298.
- (35) Strauch, S.; McLendon, G.; McGuire, M.; Guarr, T. *J. Phys. Chem.* **1983**, 87, 3579–3581.
- (36) Dorfman, R. C.; Lin, Y.; Fayer, M. D. *J. Phys. Chem.* **1989**, 93, 6388–6396.
- (37) Lin, Y.; Dorfman, R. C.; Fayer, M. D. *J. Chem. Phys.* **1989**, 90, 159–170.
- (38) Ponce, A.; Gray, H. B.; Winkler, J. R. *J. Am. Chem. Soc.* **2000**, 122, 8187–8191.
- (39) Wenger, O. S.; Leigh, B. S.; Villahermosa, R. M.; Gray, H. B.; Winkler, J. R. *Science* **2005**, 307, 99–102.
- (40) Inokuti, M.; Hirayama, F. *J. Chem. Phys.* **1965**, 43, 1978–1989.
- (41) Tachiya, M.; Mozumder, A. *Chem. Phys. Lett.* **1974**, 28, 87–89.
- (42) Blumen, A. *J. Chem. Phys.* **1980**, 72, 2632–2640.
- (43) Gurney, R. W.; Condon, E. U. *Phys. Rev.* **1929**, 33, 127–140.
- (44) Kramers, H. A. *Physica* **1934**, 1, 182–192.
- (45) Anderson, P. W. *Phys. Rev.* **1950**, 79, 350–356.
- (46) Halpern, J.; Orgel, L. E. *Discuss. Faraday Soc.* **1960**, 32–41.
- (47) McConnell, H. M. *J. Chem. Phys.* **1961**, 35, 508–515.
- (48) Oevering, H.; Paddon-Row, M. N.; Heppener, M.; Oliver, A. M.; Cotsaris, E.; Verhoeven, J. W.; Hush, N. S. *J. Am. Chem. Soc.* **1987**, 109, 3258–3269.
- (49) Beebe, J. M.; Engelkes, V. B.; Liu, J. Q.; Gooding, J.; Eggers, P. K.; Jun, Y.; Zhu, X. Y.; Paddon-Row, M. N.; Frisbie, C. D. *J. Phys. Chem. B* **2005**, 109, 5207–5215.
- (50) Wold, D. J.; Frisbie, C. D. *J. Am. Chem. Soc.* **2001**, 123, 5549–5556.
- (51) Smalley, J. F.; Finklea, H. O.; Chidsey, C. E. D.; Linford, M. R.; Creager, S. E.; Ferraris, J. P.; Chalfant, K.; Zawodzinski, T.; Feldberg, S. W.; Newton, M. D. *J. Am. Chem. Soc.* **2003**, 125, 2004–2013.
- (52) Smalley, J. F.; Feldberg, S. W.; Chidsey, C. E. D.; Linford, M. R.; Newton, M. D.; Liu, Y.-P. *J. Phys. Chem.* **1995**, 99, 13141–13149.
- (53) Newton, M. D.; Smalley, J. F. *Phys. Chem. Chem. Phys.* **2007**, 9, 555–572.
- (54) Lias, S. G.; Bartmess, J. E.; Liebman, J. F.; Holmes, J. L.; Levin, R. D.; Mallard, W. G. *J. Phys. Chem. Ref. Data* **1988**, 17, 1–861.
- (55) Bieri, G.; Burger, F.; Heilbronner, E.; Maier, J. P. *Helv. Chim. Acta* **1977**, 60, 2213–2233.
- (56) Evans, S.; Green, M. L. H.; Orchard, A. F.; Jewitt, B.; Pygall, C. F. *J. Chem. Soc., Faraday Trans. 2* **1972**, 68, 1847–1865.
- (57) Casanovas, J.; Grob, R.; Delacroix, D.; Guelfucci, J. P.; Blanc, D. *J. Chem. Phys.* **1981**, 75, 4661–4668.
- (58) *Standard Potentials in Aqueous Solution*; Bard, A. J., Parsons, R., Jordan, J., Eds.; Marcel Dekker, Inc.: New York, 1985.
- (59) Raymond, J. W.; Simpson, W. T. *J. Chem. Phys.* **1967**, 47, 430–448.
- (60) Au, J. W.; Cooper, G.; Burton, G. R.; Olney, T. N.; Brion, C. E. *Chem. Phys.* **1993**, 173, 209–239.
- (61) Costner, E. A.; Long, B. K.; Navar, C.; Jockusch, S.; Lei, X.; Zimmerman, P.; Campion, A.; Turro, N. J.; Willson, C. G. *J. Phys. Chem. A* **2009**, 113, 9337–9347.
- (62) Tachibana, S.; Morisawa, Y.; Ikehata, A.; Sato, H.; Higashi, N.; Ozaki, Y. *Appl. Spectrosc.* **2011**, 65, 221–226.
- (63) Morisawa, Y.; Tachibana, S.; Ehara, M.; Ozaki, Y. *J. Phys. Chem. A* **2012**, 116, 11957–11964.
- (64) Simons, J. *J. Phys. Chem. A* **2008**, 112, 6401–6511.
- (65) Jordan, K. D.; Burrow, P. D. *Acc. Chem. Res.* **1978**, 11, 341–348.
- (66) Jordan, K. D.; Burrow, P. D. *Chem. Rev.* **1987**, 87, 557–588.
- (67) Allan, M.; Andric, L. *J. Chem. Phys.* **1996**, 105, 3559–3558.
- (68) Liang, C.; Newton, M. D. *J. Phys. Chem.* **1992**, 96, 2855–2866.
- (69) Liang, C.; Newton, M. D. *J. Phys. Chem.* **1993**, 97, 3199–3211.
- (70) Shephard, M. J.; Paddon-Row, M. N.; Jordan, K. D. *Chem. Phys.* **1993**, 176, 289–304.
- (71) Reed, A. E.; Curtiss, L. A.; Weinhold, F. *Chem. Rev.* **1988**, 88, 899–926.
- (72) Weinhold, F. *J. Comput. Chem.* **2012**, 33, 2363–2379.
- (73) Dyke, J. M.; Ellis, A. R.; Keddar, N.; Morris, A. *J. Phys. Chem.* **1984**, 88, 2565–2569.
- (74) DePuy, C. H.; Gronert, S.; Barlow, S. E.; Bierbaum, V. M.; Damrauer, R. *J. Am. Chem. Soc.* **1989**, 111, 1968–1973.
- (75) Ruscic, B.; Berkowitz, J.; Curtiss, L. A.; Pople, J. A. *J. Chem. Phys.* **1989**, 91, 114–121.
- (76) Ratner, M. A. *J. Phys. Chem.* **1990**, 94, 4877–4883.
- (77) Davis, W. B.; Ratner, M. A.; Wasielewski, M. R. *Chem. Phys.* **2002**, 281, 333–346.
- (78) Davis, W. B.; Svec, W. A.; Ratner, M. A.; Wasielewski, M. R. *Nature* **1998**, 396, 60–63.
- (79) Eng, M. P.; Albinsson, B. *Chem. Phys.* **2009**, 357, 132–139.
- (80) Szent-Györgyi, A. *Science* **1941**, 93, 609–611.
- (81) Evans, M. G.; Gergely, J. *Biochim. Biophys. Acta* **1949**, 3, 188–197.
- (82) Kasha, M. *Rev. Mod. Phys.* **1959**, 31, 162–169.
- (83) Chance, B.; Williams, G. R. *Adv. Enzymol.* **1956**, 17, 65–134.
- (84) DeVault, D.; Chance, B. *Biophys. J.* **1966**, 6, 825–847.
- (85) Hopfield, J. J. *Proc. Natl. Acad. Sci. U.S.A.* **1974**, 71, 3640–3644.
- (86) Winkler, J. R.; Nocera, D. G.; Yocom, K. M.; Bordignon, E.; Gray, H. B. *J. Am. Chem. Soc.* **1982**, 104, 5798–5800.
- (87) Crane, B. R.; Di Bilio, A. J.; Winkler, J. R.; Gray, H. B. *J. Am. Chem. Soc.* **2001**, 123, 11623–11631.
- (88) Tezcan, F. A.; Crane, B. R.; Winkler, J. R.; Gray, H. B. *Proc. Natl. Acad. Sci. U.S.A.* **2001**, 98, 5002–5006.
- (89) Axelrod, H. L.; Abresch, E. C.; Okamura, M. Y.; Yeh, A. P.; Rees, D. C.; Feher, G. *J. Mol. Biol.* **2002**, 319, 501–515.
- (90) Gray, H. B.; Winkler, J. R. *Q. Rev. Biophys.* **2003**, 36, 341–372.
- (91) Gray, H. B.; Winkler, J. R. *Biochim. Biophys. Acta—Bioenerg.* **2010**, 1797, 1563–1572.
- (92) Winkler, J. R.; Gray, H. B. *Chem. Rev.* **2013**, DOI: 10.1021/cr4004715.
- (93) Moser, C. C.; Keske, J. M.; Warncke, K.; Farid, R. S.; Dutton, P. L. *Nature* **1992**, 355, 796–802.
- (94) Page, C. C.; Moser, C. C.; Chen, X.; Dutton, P. L. *Nature* **1999**, 402, 47–52.
- (95) Beratan, D. N.; Onuchic, J. N.; Hopfield, J. J. *J. Chem. Phys.* **1987**, 86, 4488–4498.
- (96) Onuchic, J. N.; Beratan, D. N. *J. Chem. Phys.* **1990**, 92, 722–733.
- (97) Beratan, D. N.; Onuchic, J. N.; Winkler, J. R.; Gray, H. B. *Science* **1992**, 258, 1740–1741.
- (98) Skourtis, S. S.; Balabin, I.; Kawatsu, T.; Beratan, D. N. *Proc. Natl. Acad. Sci. U.S.A.* **2005**, 102, 3552–3557.
- (99) Prytkova, T. R.; Kurnikov, I. V.; Beratan, D. N. *Science* **2007**, 315, 622–625.
- (100) Balabin, I. A.; Beratan, D. N.; Skourtis, S. S. *Phys. Rev. Lett.* **2008**, 101.

- (101) Gehlen, J. N.; Daizadeh, I.; Stuchebrukhov, A. A.; Marcus, R. A. *Inorg. Chim. Acta* **1996**, *243*, 271–282.
- (102) Stuchebrukhov, A. A. *J. Chem. Phys.* **1996**, *105*, 10819–10829.
- (103) Stuchebrukhov, A. A. *J. Chem. Phys.* **1996**, *104*, 8424–8432.
- (104) Stuchebrukhov, A. A. *Adv. Chem. Phys.* **2001**, *118*, 1–44.
- (105) Medvedev, E. S.; Stuchebrukhov, A. A. *Chem. Phys.* **2004**, *296*, 181–192.
- (106) Prytkova, T. R.; Kurnikov, I. V.; Beratan, D. N. *J. Phys. Chem. B* **2005**, *109*, 1618–1625.
- (107) Wohlthat, S.; Solomon, G. C.; Hush, N. S.; Reimers, J. R. *Theor. Chem. Acc.* **2011**, *130*, 815–828.
- (108) Lewis, F. D.; Wasielewski, M. R. *Top. Cur. Chem.* **2004**, *236*, 45–65.
- (109) Lewis, F. D. *Isr. J. Chem.* **2013**, *53*, 350–365.
- (110) Barton, J. K.; Olmon, E. D.; Sontz, P. A. *Coord. Chem. Rev.* **2011**, *255*, 619–634.
- (111) Klasinc, L. *J. Electron Spectrosc. Relat. Phenom.* **1976**, *8*, 161–164.
- (112) Plekan, O.; Feyer, V.; Richter, R.; Coreno, M.; Prince, K. C. *Mol. Phys.* **2008**, *106*, 1143–1153.
- (113) Cannington, P. H.; Ham, N. S. *J. Electron Spectrosc. Relat. Phenom.* **1983**, *32*, 139–151.
- (114) Aflatooni, K.; Hitt, B.; Gallup, G. A.; Burrow, P. D. *J. Chem. Phys.* **2001**, *115*, 6489–6494.
- (115) <http://www.uniprot.org/>
- (116) Burley, S. K.; Petsko, G. A. *Science* **1985**, *229*, 23–28.
- (117) Karlin, S.; Zhu, Z. Y.; Baud, F. *Proc. Natl. Acad. Sci. U.S.A.* **1999**, *96*, 12500–12505.
- (118) Thomas, A.; Meurisse, R.; Charletoaux, B.; Brasseur, R. *Proteins—Struct., Funct. Genet.* **2002**, *48*, 628–634.
- (119) Lanzarotti, E.; Biekofsky, R. R.; Estrin, D. A.; Marti, M. A.; Turjanski, A. G. *J. Chem. Inf. Model.* **2011**, *51*, 1623–1633.
- (120) Yau, W.-M.; Wimley, W. C.; Gawrisch, K.; White, S. H. *Biochemistry* **1998**, *37*, 14713–14718.
- (121) Hong, H. D.; Park, S.; Jimenez, R. H. F.; Rinehart, D.; Tamm, L. K. *J. Am. Chem. Soc.* **2007**, *129*, 8320–8327.
- (122) Ulmschneider, M. B.; Sansom, M. S. P. *Biochim. Biophys. Acta—Biomembr.* **2001**, *1512*, 1–14.
- (123) Shih, C. Ph.D. Thesis, California Institute of Technology, 2008.
- (124) Warren, J. J.; Ener, M. E.; Vlček, A.; Winkler, J. R.; Gray, H. B. *Coord. Chem. Rev.* **2012**, *256*, 2478–2487.
- (125) Ortega, J. M.; Mathis, P. *Biochemistry* **1993**, *32*, 1141–1151.
- (126) Deisenhofer, J.; Epp, O.; Miki, K.; Huber, R.; Michel, H. *Nature* **1985**, *318*, 618–624.
- (127) Deisenhofer, J.; Epp, O.; Sinning, I.; Michel, H. *J. Mol. Biol.* **1995**, *246*, 429–457.
- (128) Alric, J.; Lavergne, J.; Rappaport, F.; Verméglio, A.; Matsuura, K.; Shimada, K.; Nagashima, K. V. P. *J. Am. Chem. Soc.* **2006**, *128*, 4136–4145.
- (129) Voigt, P.; Knapp, E. W. *J. Biol. Chem.* **2003**, *278*, 51993–52001.
- (130) Chen, I.-P.; Pathis, P.; Koepke, J.; Michel, H. *Biochemistry* **2000**, *39*, 3592–3602.
- (131) Li, L.; Mustafi, D.; Fu, Q.; Tereshko, V.; Chen, D. L.; Tice, J. D.; Ismagilov, R. F. *Proc. Natl. Acad. Sci. U.S.A.* **2006**, *103*, 19243–19248.
- (132) Roessler, M. M.; King, M. S.; Robinson, A. J.; Armstrong, F. A.; Harmer, J.; Hirst, J. *Proc. Natl. Acad. Sci. U.S.A.* **2010**, *107*, 1930–1935.
- (133) Stubbe, J.; Nocera, D. G.; Yee, C. S.; Chang, M. C. Y. *Chem. Rev.* **2003**, *103*, 2167–2201.
- (134) Sjöberg, B. M. *Struct. Bonding (Berlin)* **1997**, *88*, 139–173.
- (135) Stubbe, J.; van der Donk, W. A. *Chem. Rev.* **1998**, *98*, 705–762.
- (136) Argirevic, T.; Riplinger, C.; Stubbe, J.; Neese, F.; Bennati, M. J. *Am. Chem. Soc.* **2012**, *134*, 17661–17670.
- (137) Holder, P. G.; Pizano, A. A.; Anderson, B. L.; Stubbe, J.; Nocera, D. G. *J. Am. Chem. Soc.* **2012**, *134*, 1172–1180.
- (138) Offenbacher, A. R.; Minnihan, E. C.; Stubbe, J.; Barry, B. A. *J. Am. Chem. Soc.* **2013**, *135*, 6380–6383.
- (139) Worsdorfer, B.; Conner, D. A.; Yokoyama, K.; Livada, J.; Seyedasayamdost, M.; Jiang, W.; Silakov, A.; Stubbe, J.; Bollinger, J. M.; Krebs, C. J. *Am. Chem. Soc.* **2013**, *135*, 8585–8593.
- (140) Yokoyama, K.; Smith, A. A.; Corzilius, B.; Griffin, R. G.; Stubbe, J. *J. Am. Chem. Soc.* **2011**, *133*, 18420–18432.
- (141) Offenbacher, A. R.; Burns, L. A.; Sherrill, C. D.; Barry, B. A. *J. Phys. Chem. B* **2013**, *117*, 8457–8468.
- (142) Chang, M. C. Y.; Yee, C. S.; Nocera, D. G.; Stubbe, J. *J. Am. Chem. Soc.* **2004**, *126*, 16702–16703.
- (143) Boussac, A.; Rappaport, F.; Brettel, K.; Sugiura, M. *J. Phys. Chem. B* **2013**, *117*, 3308–3314.
- (144) Keough, J. M.; Zuniga, A. N.; Jenson, D. L.; Barry, B. A. *J. Phys. Chem. B* **2013**, *117*, 1296–1307.
- (145) Sjöholm, J.; Styring, S.; Havelius, K. G. V.; Ho, F. M. *Biochemistry* **2012**, *51*, 2054–2064.
- (146) Tommos, C.; Babcock, G. T. *Biochim. Biophys. Acta—Bioenerg.* **2000**, *1458*, 199–219.
- (147) Sancar, A. *Chem. Rev.* **2003**, *103*, 2203–2238.
- (148) Taylor, J. S. *Acc. Chem. Res.* **1994**, *27*, 76–82.
- (149) Li, Y. F.; Heelis, P. F.; Sancar, A. *Biochemistry* **1991**, *30*, 6322–6329.
- (150) Aubert, C.; Mathis, P.; Eker, A. P. M.; Brettel, K. *Proc. Natl. Acad. Sci. U.S.A.* **1999**, *96*, 5423–5427.
- (151) Byrdin, M.; Eker, A. P. M.; Vos, M. H.; Brettel, K. *Proc. Natl. Acad. Sci. U.S.A.* **2003**, *100*, 8676–8681.
- (152) Kodali, G.; Siddiqui, S. U.; Stanley, R. J. *J. Am. Chem. Soc.* **2009**, *131*, 4795–4807.
- (153) Lukacs, A.; Eker, A. P. M.; Byrdin, M.; Villette, S.; Pan, J.; Brettel, K.; Vos, M. H. *J. Phys. Chem. B* **2006**, *110*, 15654–15658.
- (154) Woiczikowski, P. B.; Steinbrecher, T.; Kubař, T.; Elstner, M. *J. Phys. Chem. B* **2011**, *115*, 9846–9863.
- (155) Aubert, C.; Vos, M. H.; Mathis, P.; Eker, A. P. M.; Brettel, K. *Nature* **2000**, *405*, 586–590.
- (156) Davidson, V. L.; Liu, A. M. *Biochim. Biophys. Acta—Proteins Proteomics* **2012**, *1824*, 1299–1305.
- (157) Geng, J. F.; Dornevil, K.; Davidson, V. L.; Liu, A. M. *Proc. Natl. Acad. Sci. U.S.A.* **2013**, *110*, 9639–9644.
- (158) Yukl, E. T.; Liu, F. G.; Krzystek, J.; Shin, S.; Jensen, L. M. R.; Davidson, V. L.; Wilmot, C. M.; Liu, A. M. *Proc. Natl. Acad. Sci. U.S.A.* **2013**, *110*, 4569–4573.
- (159) Davidson, V. L.; Wilmot, C. M. *Annu. Rev. Biochem.* **2013**, *82*, 531–550.
- (160) Jiang, N.; Kuznetsov, A.; Nocek, J. M.; Hoffman, B. M.; Crane, B. R.; Hu, X. Q.; Beratan, D. N. *J. Phys. Chem. B* **2013**, *117*, 9129–9141.
- (161) Seifert, J. L.; Pfister, T. D.; Nocek, J. M.; Lu, Y.; Hoffman, B. M. *J. Am. Chem. Soc.* **2005**, *127*, 5750–5751.
- (162) Shih, C.; Museth, A. K.; Abrahamsson, M.; Blanco-Rodriguez, A. M.; Di Bilio, A. J.; Sudhamsu, J.; Crane, B. R.; Ronayne, K. L.; Towrie, M.; Vlček, A.; Richards, J. H.; Winkler, J. R.; Gray, H. B. *Science* **2008**, *320*, 1760–1762.
- (163) Warren, J. J.; Herrera, N.; Hill, M. G.; Winkler, J. R.; Gray, H. B. *J. Am. Chem. Soc.* **2013**, *135*, 11151–11158.
- (164) Yosca, T. H.; Rittle, J.; Krest, C. M.; Onderko, E. L.; Silakov, A.; Calixto, J. C.; Behan, R. K.; Green, M. T. *Science* **2013**, *342*, 825–829.
- (165) Schünemann, V.; Lendzian, F.; Jung, C.; Contzen, J.; Barra, A. L.; Sligar, S. G.; Trautwein, A. X. *J. Biol. Chem.* **2004**, *279*, 10919–10930.
- (166) Jung, C.; Schünemann, V.; Lendzian, F. *Biochem. Biophys. Res. Commun.* **2005**, *338*, 355–364.
- (167) Rutherford, A. W.; Osyczka, A.; Rappaport, F. *FEBS Lett.* **2012**, *586*, 603–616.
- (168) Dance, Z. E. X.; Ahrens, M. J.; Vega, A. M.; Ricks, A. B.; McCamant, D. W.; Ratner, M. A.; Wasielewski, M. R. *J. Am. Chem. Soc.* **2008**, *130*, 830–832.
- (169) Nealson, K. H.; Saffarini, D. *Annu. Rev. Microbiol.* **1994**, *48*, 311–343.

(170) Gorby, Y. A.; Yanina, S.; McLean, J. S.; Rosso, K. M.; Moyles, D.; Dohnalkova, A.; Beveridge, T. J.; Chang, I. S.; Kim, B. H.; Kim, K. S.; Culley, D. E.; Reed, S. B.; Romine, M. F.; Saffarini, D. A.; Hill, E. A.; Shi, L.; Elias, D. A.; Kennedy, D. W.; Pinchuk, G.; Watanabe, K.; Ishii, S. i.; Logan, B.; Nealson, K. H.; Fredrickson, J. K. *Proc. Natl. Acad. Sci. U.S.A.* **2006**, *103*, 11358–11363.

(171) Malvankar, N. S.; Vargas, M.; Nevin, K. P.; Franks, A. E.; Leang, C.; Kim, B.-C.; Inoue, K.; Mester, T.; Covalla, S. F.; Johnson, J. P.; Rotello, V. M.; Tuominen, M. T.; Lovley, D. R. *Nat. Nanotechnol.* **2011**, *6*, 573–579.

(172) Polizzi, N. F.; Skourtis, S. S.; Beratan, D. N. *Faraday Discuss.* **2012**, *155*, 43–62.